AIAA JOURNAL
Vol. 33, No. 4, April 1995

Wind-Tunnel Tests of an Inclined Cylinder Having Helical Grooves

Thomas D. Stuart*
United States Navy, Arlington, Virginia 22202
James M. Clifton†
Naval Air Warfare Center Aircraft Division, Patuxent River, Maryland 20670
and
Louis V. Schmidt‡
Naval Postgraduate School, Monterey, California 93943

A series of low-speed wind-tunnel investigations were conducted to determine the aerodynamic behavior of a helically grooved inclined cylinder representing a long trailing wire antenna towed from an orbiting aircraft. The large test angle-of-attack range of the wire required two model configurations. For higher angles of attack, full-scale wires were tested. For lower angles of attack, a 15-scale grooved, cylindrical model with an ogive nose was tested. Data were evaluated and empirical relationships for the normal and axial force coefficients were verified by comparison with historical references for the baseline clean circular cylinders and were extended for the grooved configurations. The existence of a side force coefficient due to circulation caused by the helical grooves was discovered, expressed analytically, and verified with flow-visualization techniques. The experimental coefficients were used to improve an existing digital simulation model describing the static-equilibrium conditions of a long cable towed by an aircraft. Inclusion of the side force influence in the static model proved consistent with flight-test observations of the wire's lateral skew angle and direction.

Nomenclature

A	= axial force
C_A	= axial force coefficient, $A/Qd\ell$
C_D	= drag coefficient
$C_{D,\text{basic}}$	= reference drag coefficient
C_f	= frictional coefficient
C_L	= lift coefficient
C_{m_α}	= pitching moment coefficient derivative with respect to angle of attack
C_N	= normal force coefficient, $N/Qd\ell$
C_{N_α}	= normal force coefficient derivative with respect to angle of attack
C_Y	= side force coefficient, $S/Qd\ell$
d	= reference body diameter
ℓ	= reference body length
N	= normal force
Q	= dynamic pressure
Re	= Reynolds number
S	= side force
T_α	= orthogonal transformation matrix
α	= angle of attack
ϕ	= roll orientation angle

Introduction

THE use of wires in the field of aeronautics started well before the Wright Flyer took to the air. Initially, wires were used as structural support for biwing gliders, and their use extended to powered biplanes. With their implementation came experimental studies and tests. One of the earliest studies of smooth and stranded wires was conducted in 1917 by Relf and Powell.[1] The later work by Hoerner[2] in 1958 relative to fluid dynamic drag has been accepted as the historical baseline in the experimental study of wires. Hoerner presents empirical relationships for the lift and drag of inclined wires, cables, and cylinders at subcritical Reynolds number ranges of 10^4–10^5. In a body-axis system for an inclined wire (Fig. 1), the normal and axial force coefficients are determined from the forces perpendicular to and parallel to the wire, respectively. The C_L and C_D force coefficients which are in a stability axis reference frame relative to the freestream velocity can be found by applying an orthogonal transformation to C_N and C_A as shown in Eq. (1).

$$\begin{Bmatrix} C_L \\ C_D \end{Bmatrix} = \begin{bmatrix} \cos\alpha & -\sin\alpha \\ \sin\alpha & \cos\alpha \end{bmatrix} \begin{Bmatrix} C_N \\ C_A \end{Bmatrix} = [T_\alpha] \begin{Bmatrix} C_N \\ C_A \end{Bmatrix} \tag{1}$$

In the context of Eq. (1), Hoerner curve fit an empirical relation to a summary plot, Fig. 2, of experimental data to obtain

$$C_A = 0$$

$$C_N = C_{D,\text{basic}} \sin^2\alpha$$

and since there was no axial force term available to provide a drag coefficient value at $\alpha = 0$, he included a ΔC_D term to finally yield

$$\begin{gathered} C_L = C_N \cos\alpha = C_{D,\text{basic}} \sin^2\alpha \cos\alpha \\ C_D = C_N \sin\alpha + \Delta C_D = C_{D,\text{basic}} \sin^3\alpha + \Delta C_D \\ C_{D,\text{basic}} = 1.1 \\ \Delta C_D = \pi C_f = 0.02 \end{gathered} \tag{2}$$

In 1970, Bootle[3] extended Hoerner's expressions to supercritical Reynolds numbers at low Mach numbers. The critical Reynolds number range, according to Prandtl and Tietjens,[4] for a clean circular cylinder in normal flow is the region of Re between 2×10^5 and 5×10^5 and represents the transition of drag coefficient from $C_D = 1.2$ to a lower value of $C_D = 0.3$. It is generally accepted that flow in the subcritical Reynolds number region corresponds to a circular cylinder experiencing laminar flow separation whereas supercritical Reynolds numbers are associated with flow separation of a turbulent boundary layer.

Received July 8, 1993; presented as Paper 93-3456 at the AIAA 11th Applied Aerodynamics Conference, Monterey, CA, Aug. 9–11, 1993; revision received June 30, 1994; accepted for publication Aug. 1, 1994.

*Lieutenant Commander. Senior Member AIAA.
†Lieutenant Commander, United States Navy. Senior Member AIAA.
‡Professor Emeritus, Department of Aeronautics and Astronautics. Associate Fellow AIAA.

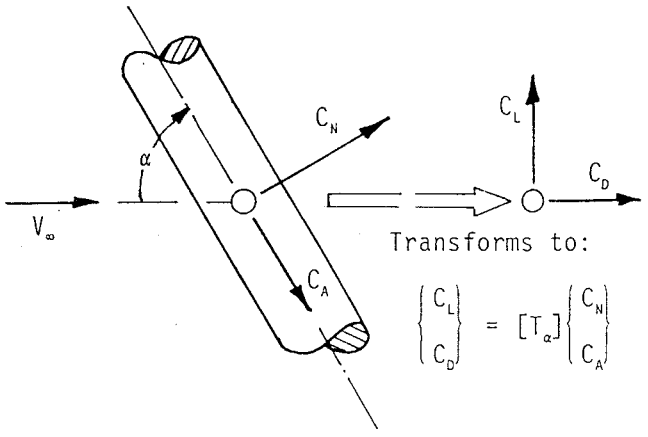

Fig. 1 Inclined wire coordinate system.

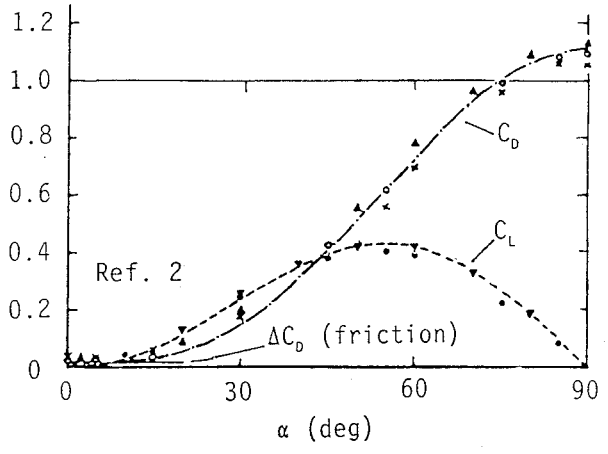

Fig. 2 Hoerner's summary of inclined wire C_D and C_L.

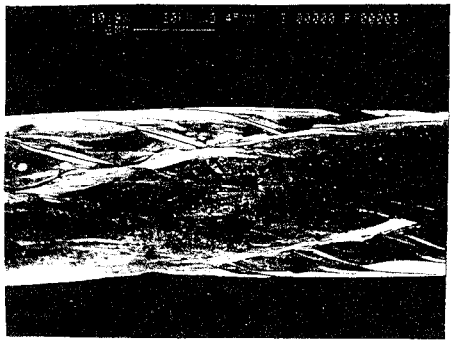

Fig. 3 Side view of 3 × 7 wire.

More recent studies have focused on critical and supercritical flow over slender, axisymmetric, finite-length bodies in response to interest in missile-related aerodynamics. Studies by Almosnino and Rom[5] using a sting balance supported cone-cylinder model examined the magnitude of the side force coefficient C_Y at higher angles of attack and the effect of symmetric blowing from the nose cone on the alleviation of side force. Vortex-induced side force investigations continued with high angle-of-attack studies by Reding and Ericsson.[6] An appraisal to experimental results led to their position that the maximum side force, on an order of magnitude equal to the cylinder's normal force, could occur in the critical Reynolds number range due to the development of an asymmetrical separation pattern. Murthy and Rose[7] addressed vortex separation points by the measurement of the skin friction coefficient. Current research addresses vortex induced separation and side forces, as applied to missiles, at high angles of attack and high Reynolds numbers.

This paper examines the side forces generated by helical grooves on an infinite cylinder, representative of a wrapped inclined wire, at low angles of attack and subcritical Reynolds numbers (i.e., Re from 4×10^3 to 2×10^5) where the C_D of an unyawed ($\alpha = 90$ deg), smooth circular cylinder has an approximate constant value of 1.2.

The motivation for these studies was related to improved modeling of the nonlinear, oscillatory dynamics displayed by a long wire trailed from an orbiting aircraft. Recent studies by Clifton[8] and Clifton et al.[9] have resulted in both a system model and viable numerical solutions to the trailing-wire dynamics. The foundation of the Clifton model is the TAC17 computer simulation that provides no-wind, static-equilibrium solutions of a trailing wire and drogue system for a given tow plane altitude, airspeed, and bank angle. Accuracy of the Clifton model was only limited by the use of approximate aerodynamic coefficients for the test wire.

The test wire that was used to generate a set of flight-test data was defined as the 3 × 7 wire which corresponds to three sets of seven symmetrically placed steel wires embedded in a copper sheath and wrapped to form a single bundle. The final 0.40-cm-(0.158 in.-) diam wire had a triple helix groove with 4.75-cm (1.87-in.) pitch and 15-deg angle (Fig. 3). With a length of up to 7620 m (25,000 ft), the 3 × 7 wire flew in an aerodynamic environment with altitudes from 910 to 6100 m (3000 to 20,000 ft), airspeeds from 18 m/s to more than 115 m/s (60 to 375 ft/s) and angles of attack relative to the velocity vector ranging from 10 to 90 degs. Corresponding operating Reynolds numbers varied between 3.5×10^3 to 1.8×10^4 along the length of the trailing wire.

Discussion

Experimental Setup and Procedures

The experiments were conducted by Stuart[10] in the Naval Postgraduate School's low-speed, closed-circuit wind tunnel. The test section was 114 cm wide, 71 cm high, and 122 cm long. Tunnel velocities ranged from 15 to 70 m-s^{-1} with a typical test-section turbulence level of 0.2%. Two balance systems were used to test the models in the angle-of-attack range of interest.

An external, four-component, reflection-plane (wall) balance was used to measure normal and axial forces of the full scale 3 × 7 wire array. Six 30 cm-lengths of the 3 × 7 wire were tightly suspended and spaced 5.1 cm apart between 1.59-cm-diam steel drill rod stanchions having 34.3 cm length and mounted vertically on a 39.7-cm-diam turntable (Fig. 4). The length-to-diameter ratio for each of the six parallel models corresponded to 75 and 38 for the 3 × 7 wires and the drill rods, respectively. These ratios were the basis for considering the test data as closely representing infinite cylinder results. Tares to account for the support system were obtained by testing with the wires removed. The wire length was in excess of 19 stanchion diameters which tended to keep stanchion/wire junction aerodynamic interference of secondary import for angles of attack greater than about 30 deg. The spacing between the parallel wire/cylinder models corresponds to 12.8 and 6.5 diameters for the 3 × 7 wires and the 0.79-cm-diam drill rods, respectively. With this lateral spacing, mutual flowfield velocity interference between adjacent models was considered as negligible (less than 0.6%) based upon classical potential flow analysis. Neither the 3 × 7 wire nor the drill rod installations exhibited any tendency of vibrate during the testing.

Strain-gauge bridge outputs from the wall balance were signal conditioned and digitally sampled at 1770 Hz followed by averaging

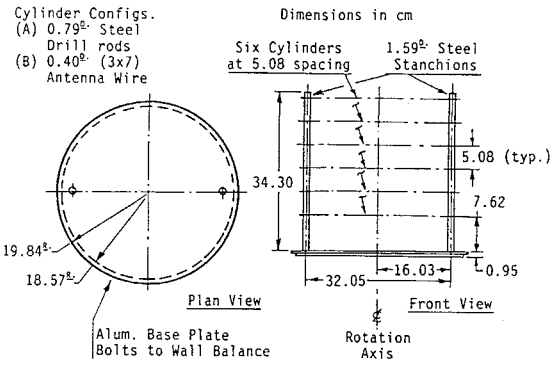

Fig. 4 Sketch of wall-balance model.

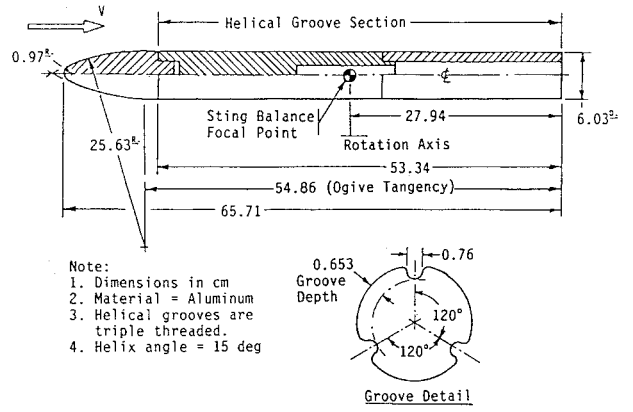

Fig. 5 Sketch of sting-balance model.

every 1000 samples for each data point. Balance sensitivity was approximately ±0.18 N (±0.04 lb) for both the normal and axial forces which translated to a ΔC_N or ΔC_A sensitivity of ±0.016 and ±0.008 for the 3 × 7 wire and drill rods, respectively, at a representative Q of 1440 N/m^2 (30 psf). The Reynolds number based on the 3 × 7 wire diameter was 1.3 × 10^4 at this value of Q. Tests were conducted with dynamic pressures Q from 480 to 2870 N/m^2 (10 to 60 psf) and angles of attack from −15 to 105 deg to best cover the subcritical range of Reynolds numbers encountered by the wire during flight operations. Correlation of the system was obtained by replacing the 3 × 7 wires with 0.79-cm-diam polished-steel drill rods and comparing the drag coefficient results with known clean cylinder data.

The estimated experimental uncertainties in the wall-balance data (due to random errors) at $Q = 1440 \pm 10$ N/m^2 were $\Delta C_N = \pm 0.010$ and ±0.020 for the drill rods and 3 × 7 wires, respectively, whereas $\Delta\alpha = \pm 0.06$ deg. All uncertainties are cited at 20:1 odds as described by Beckwith et al.[11]

The second configuration included a six-component, 2.54-cm-diam, Mark XIV, internal TASK® balance used with a sting support system constrained between the wall-balance turntable and the test-section ceiling. The model was located on the test-section centerline. Since the rotation axis was vertical, angle of attack changes took place in a horizontal plane. The sting support's symmetry axis had a tilt from the horizontal of −1.6 deg (nose downward) which resulted in a slight bias or offset in the aerodynamic side force of the model. The balance supported a 53.3-cm-long, 6.0-cm-diam aluminum cylinder with a 12.4-cm-long, two-caliber tangent ogive nose (Fig. 5). The sting balance's focal point was located on the model's rotation axis which maintained the center of the model approximately in a constant test-section flowfield. Data acquisition was similar to that described for the wall-balance system. Balance sensitivity for ΔC_N, ΔC_A, and ΔC_Y was approximately ±0.022, ±0.003, and ±0.014, respectively for the 3 × 7 wire at a representative Q of 1440 N/m^2. Models included a baseline clean cylinder, a 15-scale, right-helix model representative of the 3 × 7 wire and a left-helix model (opposite helix direction). The model's length constraint due to the tunnel size resulted in the model's helix pattern being 75% of a complete spiral. For this reason, the tests were repeated sequentially with the model rotated in 90-deg increments about the axis of symmetry to asses the influence of the finite helix spiral groove pattern. In addition, a 1.2-cm-wide strip of 220 grit sandpaper was attached circumferentially at the base of the ogive nose to reduce the influence of nose-generated asymmetric flow separation at higher angles of attack.[12] Tests were conducted for an angle of attack range of ±50 deg at values of Q from 960 to 2390 N/m^2 (20 to 60 psf) with corresponding Reynolds numbers ranging from 1.63 × 10^5 to 2.57 × 10^5.

The estimated experimental uncertainties in the sting-balance data (due to random errors) at $Q = 1915 \pm 15$ N/m^2 were $\Delta C_N = \pm 0.015$, $\Delta C_A = \pm 0.003$, and $\Delta C_Y = \pm 0.010$.

Normal Force

Normal force measurements obtained from the wall-balance model for both the 3 × 7 wires and drill rods showed only a slight

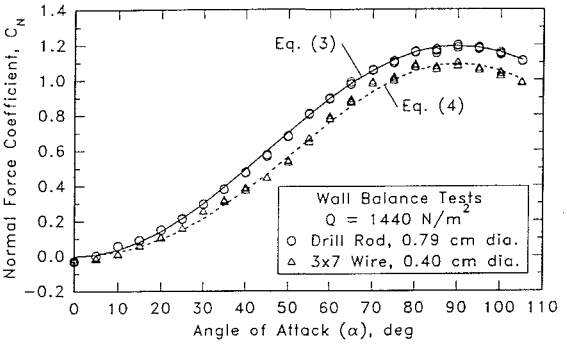

Fig. 6 Wall-balance C_N summary; uncertainty in $C_N = \pm 0.010$ (o), ± 0.020 (Δ), and $\alpha = \pm 0.06$ deg.

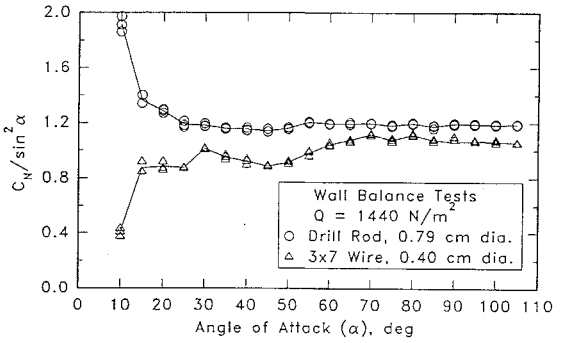

Fig. 7 C_N normalized relative to crossflow velocity; uncertainty in $C_N = \pm 0.010$ (o), ± 0.020 (Δ), and $\alpha = \pm 0.06$ deg.

variation in C_N with change in dynamic pressure in the subcritical Reynolds number range under investigation. Figure 6 shows C_N as a function of angle of attack (α) for both the 3 × 7 wire and the drill rod at a Q of 1440 N/m^2. The clean circular cylinder (polished drill rod) value of C_N at $\alpha = 90$ deg was evaluated as 1.193 ± 0.010 which agreed quite well with the accepted value[4] of $C_D = 1.20$ for an infinite circular cylinder in the subcritical Reynolds number range. Although the value of $C_{D,\text{basic}} = 1.1$ in Eq. (2) was given by Hoerner[2] as an average value to be used without any distinction as to the wire or cylinder cross section for describing the influence of angle of attack, values of C_D were cited in the subcritical Reynolds number range of 10^4–10^5 as 1.19 for a clean circular cylinder, $C_D = 1.14$ for an 0.33-cm-diam. wire containing 120.7-mm-diam wires in the outer wrap and $C_D = 1.04$ for an 0.37-cm-diam wire having five 0.13-cm-diam outer wrap wires. The experimentally determined value of $C_N = 1.090 \pm 0.020$ at $\alpha = 90$ deg for the 3 × 7 wire appears as in good accord with Hoerner's cited values.

Hoerner[2] proposed that in the subcritical Reynolds number range only the component of velocity normal to the cylinder is responsible for the flow and the aerodynamic forces experienced by infinite circular-cylinder and wire-like bodies. This assumption implied that the axial velocity component along the cylinder has, at best, a small influence on the nature of the flow separation on an infinite length cylinder or wire. The normal force coefficient, when normalized to the normal velocity component, can be represented by $C_N/\sin^2\alpha$, and this quantity should remain approximately invariant with angle of attack according to Hoerner. The $C_N/\sin^2\alpha$ term is shown in Fig. 7 using the data of Fig. 6 for both the clean drill rod and 3 × 7 wire models for various values of α except the singular value at $\alpha = 0$ deg. It will be noted that the clean cylinder results are in approximate agreement with Hoerner's supposition in the α range from 25 through 90 deg. The departure from the crossflow assumption at values of α below 25 deg can be partially attributed to stanchion/wire junction aerodynamic interference. Consequently, data accuracy was considered as unreliable for values of α below 25 deg on both model configurations when tested on the reflection plane setup. The 3 × 7 wire data shown on Fig. 7 obeyed the cross flow assumption at the higher α values but deviated low in the midrange of angles of attack. An interpretation of this observation is that the axial

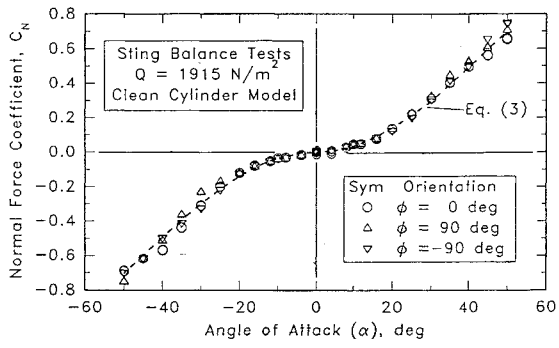

Fig. 8 Sting balance C_N for clean cylinder model; uncertainty in C_N = ±0.015 and α = ±0.06 deg.

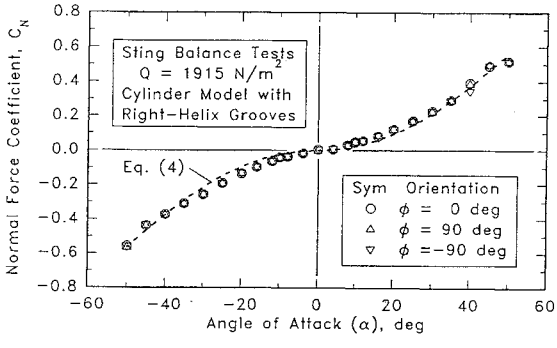

Fig. 9 Sting balance C_N for cylinder model with right-helix grooves; uncertainty in C_N = ±0.015 and α = ±0.06 deg.

velocity for this specific wire configuration did influence the nature of the crossflow, an effect not apparent on smooth cylinders and possibly also on wires with more shallow wire-wrap helix angles. An empirical curve fit for the C_N variation with α in the subcritical Reynolds number range can be described by

$$C_N(\alpha) = 1.193 \sin^2 \alpha \tag{3}$$

for the clean cylinder and

$$C_N(\alpha) = 1.09 \sin^2 \alpha - 0.08 \sin^2(2\alpha) \tag{4}$$

for the 3 × 7 wire.

The reference area used for the sting-balance models was arbitrarily set to represent the helical-groove section (53.3 × 6.0 cm) for the first part of the investigations and finally adjusted based on logic described subsequently. The normal force coefficient C_N dependence on α was found to be invariant for tested Q values between 958 and 1915 N/m^2. In addition, rotation of the model in 90-deg increments did not alter the variation of C_N with angle of attack, and the use of sandpaper in the nose region as described earlier also had little influence on C_N. The reference area finally used in analyzing the sting-balance data was an increase by 25% from the first value to reflect better the presence of the nose ogive section in the development of normal force. A clue as to the nose influence was obtained from a consideration of the sting model's C_{N_α} and C_{m_α} values at α = 0 deg which indicated that the model's aerodynamic center was forward of the balance focal point by approximately 0.8 cylinder diameters. Changing the sting-balance model's reference area from 320 to 400 cm^2 had an added benefit in that C_N values then had reasonable agreement with those obtained from the wall-balance model in the 45-deg angle-of-attack region. A comparison of the experimentally determined, clean-cylinder C_N results with Eq. (3) is shown in Fig. 8. The agreement in curve shape and magnitude is good, thereby providing further support for the final selection of a reference area when establishing the dimensionless aerodynamic coefficients.

A similar comparison between experiments on the right-helix sting-balance model and the corresponding empirical relation Eq. (4) may be seen in Fig. 9. The agreement between the experimental results and Eq. (4) in the angle-of-attack region of 30–50 deg

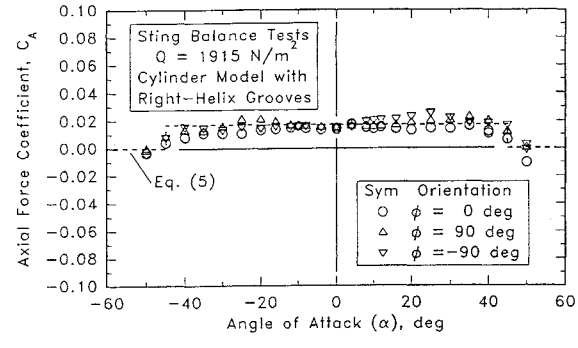

Fig. 10 Sting balance C_A for cylinder model with right-helix grooves; uncertainty in C_A = ±0.003 and α = ±0.06 deg.

is reasonable. However, the larger experimental values of C_N in the α region of 0–30 deg suggests that the aerodynamic influence of the triple-helix spiral grooves was not fully developed at low angles of attack. The variation of C_N with α was also obtained for the model with a left-helix spiral groove pattern; however, the results did not differ from those of its image configuration (model with right-helix spiral grooves).

Axial Force

Axial force coefficients from the wall-balance experiments were inconclusive since the angle-of-attack range where data could be considered as reliable (α = 30–90 deg) resulted in C_A values being of the same order of magnitude as the wall-balance sensitivity. Axial force measurements from the sting-balance model, although small in value, were consistent and reasonable with respect to balance sensitivity. C_A as a function of α for the right-helix model is shown in Fig. 10. Based on these trends, an empirical relation was estimated as shown by Eq. (5). The magnitude of C_A is considered as consistent with Hoerner's estimate[2] as shown in Eq. (2). Defining a zero value for C_A in the higher α range was based on the fact that the axial force must vanish at α = 90 deg. Since the value of C_A determined from the sting-balance model did not exhibit a functional variation as well defined as that found for C_N, the use of constants to represent a skin friction influence was assumed.

$$C_A = \begin{cases} 0.017 \text{ for } 0 \le \alpha \le 45 \text{ deg} \\ 0.0 \text{ for } 45 \le \alpha \le 90 \text{ deg} \end{cases} \tag{5}$$

Side Force

Side force measurements from the sting-balance test sequence were used to evaluate the dependence of C_Y on angle of attack. Repeated tests with the model rotated each time about the symmetry axis in 90-deg increments disclosed little C_Y variation in the ±20-deg α range for the clean cylinder and the ±12-deg α range for the helical grooved models. The 220 grit sandpaper strip on the model's nose tended to settle the larger C_Y values at higher values of α for the clean cylinder but displayed little influence on the helically grooved models. This latter independence tended to highlight the aerodynamic influence of the helical grooves over possible asymmetric vortex shedding from the tangent-ogive nose at the tested values of α. As with the normal force coefficients, C_Y values were invariant with changes in test dynamic pressure for the subcritical Reynolds number range investigated. Figures 11 and 12 show the experimentally determined dependence of C_Y on angle of attack for the clean and right-helix grooved cylinder models, respectively, including the influence of axial rotation. The center of pressure for side force was found to be within 1 cm of the balance focal point.

The influence of the helical grooves in the creation of circulation with the attendant production of side force due to crossflow was estimated by comparing the C_{Y_α} derivatives at α = 0 deg. The circulation theory was supported by flow-visualization tests. At low angles of attack, tufts on the backside of the right-helix model showed alignment to the grooves during tunnel operation. The alignment was observed only at the lower α values, whereas tuft position was dominated by direct tunnel flow at the higher angles of attack.

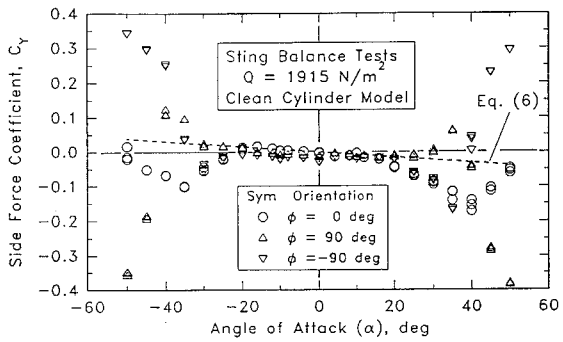

Fig. 11 Sting balance C_Y for clean cylinder model; uncertainty in C_Y = ±0.010 and α = ±0.06 deg.

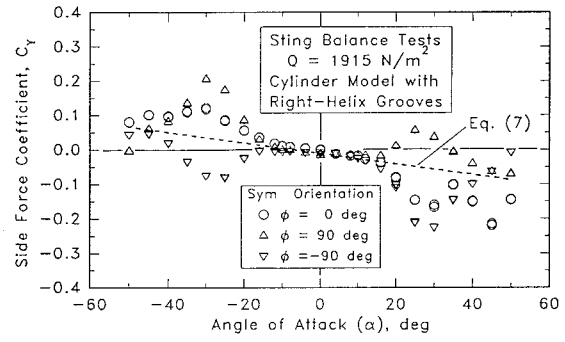

Fig. 12 Sting balance C_Y for cylinder model with right-helix grooves; uncertainty in C_Y = ±0.010 and α = ±0.06 deg.

C_{Y_α} estimates from Figs. 11 and 12 indicated that

$$C_{Y_\alpha} = -0.044 \text{ rad}^{-1} \tag{6}$$

for the clean cylinder model and

$$C_{Y_\alpha} = -0.088 \text{ rad}^{-1} \tag{7}$$

for the cylinder model with right-helix grooves.

The net change in side-force production due to the specific right-helical groove pattern was $\Delta C_{Y_\alpha} = -0.044$ rad^{-1}. The left-helix grooved model resulted in a similar positive increment in the production of side force.

Comparison of Figs. 11 and 12 combined with observations of the tufted models suggest that the influence of the helical grooves on C_Y peaked at about $\alpha = \pm 30$ deg and had a tendency to vanish at about ±50 deg. Using these facts as assumptions led to an empirical model to describe the production of C_Y due to the right-helical groove as

$$C_Y = \begin{cases} -0.0148 \sin 3\alpha & \text{for } |\alpha| \leq 60 \text{ deg} \\ 0.0 & \text{for } |\alpha| > 60 \text{ deg} \end{cases} \tag{8}$$

Comparison with Flight Tests

Flight tests using the 3 × 7 wire disclosed a surprising observation; namely, during wings-level flight the long wire trailed at an approximate 10-deg angle (to the right looking aft) from the usual straight-aft trail position observed when towing other wires having a relatively clean cylinder form. The tow plane flight conditions for the observation were 156 knots equivalent airspeed (KEAS) at an altitude of 5585 m with 0-deg bank angle. The length of the 3 × 7 wire in tow was 6069 m and terminated at the extreme end by a conically-shaped drogue. Numerical simulations used the TAC17[8,9] digital program with the aerodynamics altered to reflect the estimated 3 × 7 wire features as described by Eqs. (4), (5), and (8). The drogue was modeled using aerodynamic results obtained by Stuart.[10] The program modeled the long wire by dividing it into 200 linked segments and then iterated on an initial trial condition until static equilibrium was reached for the aerodynamic and inertial forces nonetheless matching the fixed boundary condition at the tow

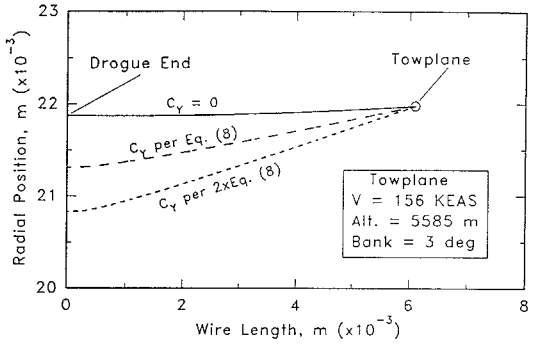

Fig. 13 C_Y influence on radial trail position.

plane. Since the TAC17 simulation program was designed to consider orbital flight by the tow plane, wings-level flight could not be modeled because of the numerical singularities caused by an infinite radius flight path. Instead, a 3-deg left-bank angle was considered for the simulation which corresponded to a flight radius of about 21,980 m (11.9 n.mi.). Although the calculated trail angle values did not apply to a wings-level flight condition, the incremental changes in trail angle were assumed as valid for illustrating the effects of altering the side force coefficient since the tow plane was nearly wings level.

When the simulation using the TAC17 program was performed without any aerodynamic side force on the wire ($C_Y = 0$), the wire trail angle at the aircraft was −2.4 deg. With C_Y activated in the program in accord with Eq. (8), the trail angle increased to −7.9 deg for a Δ angle change of −5.5 deg in the observed direction. Increasing the C_Y in Eq. (8) by a factor of two resulted in a Δ angle of −10.1 deg, which is in reasonable agreement with the flight observed behavior. A comparison showing the effect of scaling C_Y on the predicted 3 × 7 wire's radial position is shown in Fig. 13.

The use of a factor of two when describing the side force was considered reasonable because of the following factors: 1) the flight-test-observed trail angle was quantified visually not measured from instrumentation, 2) the experimental sting model represented only 3.6 cm and 0.75 revolutions of a 6096-m wire with over 130,000 spiral groove revolutions, and 3) a finite-length circular cylinder has a reduced force coefficient as compared to a cylinder of infinite length.[4,13] It is well known that the production of lift due to α on a finite wing is reduced when compared with an infinite aspect ratio wing. The production of circulation due to the grooves on the sting model does not represent the process on an infinitely long wire and, therefore, the measured results can be expected to be less from those on a wire of infinite extent. Since these investigations of a specific wire configuration are unique, correlation of the C_Y results with flight-test observations is considered only as an approximate measure of the influence of wire length on C_Y.

Conclusions

Experimentally derived C_N force coefficients for a clean cylinder at subcritical Reynolds numbers were in good accord with historical relationships.[2] Measurements of the C_N variation with angle of attack for a specific (3 × 7) wire configuration having helical groove features differed from predictions of Ref. 2 in the approximate angle-of-attack range of $0 \leq \alpha \leq 60$ deg. An added term was introduced into the numerical representation for C_N of the 3 × 7 wire to account for these differences. Although the C_A force coefficient was in approximate accord with Ref. 2 at low angles of attack, the numerical approximation was modified to be zero for $\alpha \geq 45$ deg since its influence on the total aerodynamic force was overshadowed by over three orders of magnitude relative to C_N when $\alpha \geq 45$ deg. In addition, C_A should be zero on an infinite cylinder for $\alpha = 90$ deg.

Discovered during these experiments was a side force coefficient caused by helical-groove induced flow circulation and dependent on groove direction. Small in magnitude, the side force was estimated as being present at lower wire angles of attack for the subcritical Reynolds number range considered. Computer simulations were used to verify the accuracy of the side force coefficient estimates by comparing predicted results for wire trail angle at the

tow plane with those observed in actual flight tests involving an aircraft towing a similar shaped long wire. A correction factor of two appeared reasonable to account for the differences in C_Y between the three-dimensional character of the sting-balance tests and the two-dimensional nature of the long, towed cable.

References

[1]Relf, E., and Powell, C., "Tests on Smooth and Stranded Wires Inclined to the Wind Direction, and a Comparison of Results of Stranded Wires in Air and Water," R and M 307, British Aeronautical Research Committee, England, Jan. 1917.

[2]Hoerner, S. F., *Aerodynamic Drag*, published by the author, 1958, pp. 137–139.

[3]Bootle, W., "Forces on an Inclined Circular Cylinder in Supercritical Flow," *AIAA Journal*, Vol. 9, No. 3, 1971, pp. 514–516.

[4]Prandtl, L., and Tietjens, O. G., *Applied Hydro- and Aeromechanics*, McGraw-Hill, New York, 1934, pp. 95–100.

[5]Almosnino, D., and Rom, J., "Lateral Forces on a Slender Body and Their Alleviation at High Incidence," *Journal of Spacecraft and Rockets*, Vol. 18, No. 5, 1981, pp. 393–400.

[6]Reding, J., and Ericsson, L., "Re-examination of the Maximum Normalized Vortex-Induced Side Force," *Journal of Spacecraft and Rockets*, Vol. 21, No. 5, 1984, pp. 433–440.

[7]Murthy, V., and Rose, W., "Detailed Measurements on a Circular Cylinder in Cross Flow," *AIAA Journal*, Vol. 16, No. 6, 1978, pp. 549, 550.

[8]Clifton, J. M., "Modeling and Control of a Trailing Wire Antenna Towed by an Orbiting Aircraft," Doctoral Dissertation, U.S. Naval Postgraduate School, Monterey, CA, Sept. 1992.

[9]Clifton, J. M., Schmidt, L. V., and Stuart, T. D., "Dynamic Modeling of a Trailing Wire Towed by an Orbiting Aircraft," AIAA Paper 93-3663, Aug. 1993.

[10]Stuart, T. D., "Experimental Study of the Effect of Helical Grooves on an Infinite Cylinder," Engineer's Degree Thesis, U.S. Naval Postgraduate School, Monterey, CA, Dec. 1992.

[11]Beckwith, T. G., Marangoni, R. D., and Lienhard, J. H., *Mechanical Measurements*, 5th ed., Addison-Wesley, Reading, MA, 1993, pp. 55–64.

[12]Ericsson, L., and Reding, J., "Asymmetric Flow Separation and Vortex Shedding on Bodies of Revolution," *Tactical Missile Aerodynamics: General Topics*, edited by M. J. Hemsch, Vol. 141, Progress in Astronautics and Aeronautics, AIAA, New York, 1992, pp. 391–444.

[13]Allen, H., "Estimation of the Forces and Moments acting on Inclined Bodies of Revolution of High Fineness Ratio," NACA RM A-9126, Nov. 1949.